Antibacterial effect of calcium oxide Nano-plates fabricated from Shrimp shells

Journal:	*Green Chemistry*
Manuscript ID:	GC-COM-03-2015-000615.R1
Article Type:	Communication
Date Submitted by the Author:	22-Apr-2015
Complete List of Authors:	Gedda, Gangaraju; NSYSU, Doctorial degree program in marine biotechnology Pandey, Sunil; National Sun Yet sen university, Chemistry Lin, Yu; National Sun Yet sen university, Chemistry Wu, Hui Fen; National Sun Yat-Sen University,

Antibacterial effect of calcium oxide nano-plates fabricated from shrimp shells

Gangaraju Gedda[4], Sunil Pandy[1, 5], Yu- Chih Lin[1], Hui-Fen Wu[1, 2, 3, 4, 5*]

[1]Department of Chemistry, National Sun Yat-Sen University, Kaohsiung, 70, Lien-Hai Road, Kaohsiung, 80424, Taiwan

[2]School of Pharmacy, College of Pharmacy, Kaohsiung Medical University, Kaohsiung, 807, Taiwan

[3]Institute of Medical Science and Technology, National Sun Yat-Sen University, 70, Lien-Hai Road, Kaohsiung, 80424, Taiwan

[4]Doctoral Degree Program in Marine Biotechnology, National Sun Yat-Sen University and Academia Sinica, Kaohsiung, 80424, Taiwan

[5]Center for Nanoscience and Nanotechnology, National Sun Yat-Sen University, 70, Lien-Hai Road, Kaohsiung, 80424, Taiwan

*Corresponding author, Phone: +886-7-5252000-3955; Fax: +886-7-5253909

E-mail: hwu@faculty.nsysu.edu.tw (Prof. HF Wu)

We have used shrimp shells as novel and green source of precursors to produce calcium oxide nanoplates ranging from 40 to 130 nm (in length) and 30 to 100 nm (in width). These nanoparticles were found to possess effective antimicrobial activity to against gram positive and gram-negative bacteria. The percentage yield of the CaO nano-plates (8 %) enables this method to become a highly effective industrial technique.

Due to the profound impact of the nano-scale (10-100nm) on properties of materials, nanoparticles (NPs) have become the most widely used materials for modern scientific research especially in electronic and medical sciences[1]. Many methods include microwave, hydrothermal, sol-gel, sonochemical and solvothermal have been developed to prepare various types of NPs[1, 2]. However, the majority of the protocols mentioned above required inimical materials as precursors but the process typically requires intensive purification strategies. Therefore, extensively endeavors to explore novel methods for nanoparticles synthesis toward eco-friendly and less time and process consuming are definitely required.

Among the huge variety of nanoparticles synthesized till date, the metal oxide nanoparticles, such as Al_2O_3, ZnO, MgO, CuO, TiO_2, and CaO are well known for their inherent anti-microbial activity[3]. Also, due to their high stability and unique physico-chemical properties, these nanoparticles are highly significant nano-materials in material science.

Marine crustacean, such as shrimp shells are the major by products generated by sea food industries [4]. The major chemical components of these shells contain calcium and several biomolecules such as proteins, chitin, lipids and pigments etc.[5]. Due to these important chemical constituents, shrimp shells have become a vital precursor for industrial products such as chitosan, exceptionally significant biomedical applications including anti-bacterial and anti-fungal agents, chelators to clutch metals from environmental samples[6-8]. During the industrial processing of shrimp cells, in order to extract the above mentioned chemical constituents, the raw materials are treated in such a way that majority of calcium is discarded without their active extraction for further use. The increasing demand of calcium-based nanomaterials has inspired us to use these by products as a precursor of calcium oxide nanoparticles.

Green synthesis of CaO NPs from the shrimp shell was achieved in two-step process ((Fig. S1). In the first step, the dried shrimp shell powder was treated with diluted hydrochloric acid to obtain $CaCl_2$, which was further treated with Na_2CO_3 solution in order to form $CaCO_3$. In the second step, the resulting $CaCO_3$ was subjected to calcination to deliver the desired nano-plate size CaO. The intermediate product $CaCO_3$ was characterized using various spectroscopic techniques such as UV-Visible spectroscopy, Fourier transform infrared spectroscopy (FT-IR), X-ray diffraction (XRD) spectroscopy, Energy-dispersive X-ray (EDX) spectroscopy (Fig. S2). In the UV-Vis, the aqueous $CaCO_3$ solution exhibited a strong absorption band in the range around 200 - 1000 nm with the maximum absorption at 250 nm (Fig. S2A), which has been confirmed from literature[9]. The FT-IR spectrum of the vacuum dried shrimp shells derived $CaCO_3$ was measured in the optical window between 4000 - 500 cm^{-1} (Fig. S2B), and it was in agreement with previous reports[10, 11]. The sharp peaks at 714 cm^{-1} and 873 cm^{-1} corresponding to C-O vibrational stretching and bending respectively was noticed. Further, the asymmetrical and symmetrical lengthening of the C-O-C bond was appeared at 1490 cm^{-1} followed by C=O stretching at 1799 cm^{-1}, which has unambiguously confirmed the existence of $CaCO_3$. The crystalline nature of prawn shell waste derived $CaCO_3$ was analyzed by powder XRD (Fig. S2C). A number of Bragg reflections with (2θ)

values of 23.07, 29.62, 36.18, 39.55, 43.41, 47.78, 48.62, 57.71, 61.23 and 65.10, sets of lattice planes are observed which are belongs to the (*hkl*) indices (012) (104) (110) (113) (202) (018) (116) (122) (214) and (300) facets of $CaCO_3$ calcite respectively ((JCPDS card number 72-1652)[11]. Therefore, the XRD pattern clearly demonstrates that the $CaCO_3$ formed in this present synthesis are crystalline in nature. Moreover, these results also reveal that the synthesized $CaCO_3$ was obtained in high purity, which could be attributed to the presence of large quantity of calcium in shrimp shells. The EDX analysis results provided the elemental composition of shrimp shell derived $CaCO_3$ component. The existence of strong signals in the region corresponding to Ca, C and O further confirms the formation of $CaCO_3$ (Fig. S2D). The additional appearance of Cu signal is more likely due to the copper Transmission Electron Microscopy (TEM) grids (sample holders). The above characterization results from various instrumental techniques, have confirmed unambiguously for the extraction of highly pure $CaCO_3$ from the shrimp shells.

The CaO nanoparticles were prepared by calcination of $CaCO_3$ at high temperature (900 ^oC) upon the elimination of CO_2. The synthesized nano-size CaO was characterized by using UV-Vis spectroscopy, FT- IR, XRD (Fig. S3). CaO showed a single sharp band with absorption maximum at 270 nm, which was about 20 nm bath-chromic shift compared to $CaCO_3$ as shown in fig. S3A. In spite of the large size of the nanoparticles, the stability may be conferred by counter ions or protein molecules. The stability of nanoparticles was studied for 15 days. The change in the optical absorbance (λ_{max}) was scrutinized for 15 days and there was no apparent shift in the absorbance (Table S1A). Similar experiment was performed by adding different concentration of sodium chloride in the nanoparticles solution and assessing the change in absorbance (Table S1B). These studies have confirmed the stability of nanoparticles. Fig. S3B represents the FT-IR spectrum of CaO, and it displayed wide and intense bands at 500 cm^{-1}, 1482 cm^{-1} and week band at 877 cm^{-1} corresponding to Ca-O stretching, which is in consistence with the literatures[11-13]. The peak at 3657 cm^{-1} is attributed to the absorption of -OH groups present on the surface of CaO. The XRD pattern of CaO showed a different set of diffraction peaks (2θ) at 32.02, 37.12, 53.80, 64.17 and 67.26, which are belong to the (*hkl*) indices (111) (200) (202) (311) and (222) respectively, of crystal planes (Fig. S3C) [14]. The lattice patterns were in accordance with JCPDS (card number 82-1690) CaO standard values. EDX results display elemental composition of CaO. The appearance of signals corresponding to Ca and O and especially disappearance of "C"

signals clearly confirms the formation of CaO (Fig. S3D). All the above characterization techniques proved that the $CaCO_3$ was completely transformed to CaO.

The size and shape of CaO particles were confirmed by TEM measurements and the results are displayed in Fig. 1. The TEM images reveal that the CaO particles were form uniformly dispersed nano plates (Fig. 1A and B). Fig. 1C and 1D display the size and shape distribution of CaO nanoparticles in the form of histograms. The particles with various lengths ranging from 40-130 nm (avg. length of 66 nm) and the width of 30-100 nm (avg. width 68 nm) were observed. According to earlier studies, like biological synthesis of nanoparticles, proteins have cardinal roles to modify the shapes of nanoparticles by altering their thermodynamic surface energy or specific crystal lattices[15, 16]. However, high temperature may also influence the shape transition. We can conclude the combined roles of proteins (initiation of shape transition) and higher temperature (quenching the reaction). The antibacterial activity of CaO NPs studied to against *E.coli* and *S.aureus* using growth curve and disc diffusion methods under physiological conditions (pH=7.4). For this study, various concentrations of CaO nanoplates (5 - 50 μg mL^{-1}) were added to bacterial culture suspension. The growth rate kinetic was investigated at different time intervals by measuring the cells suspension turbidity optical density at 600 nm (OD_{600}) (Fig. 2). The results revealed that in the absence of CaO NPs (control experiments), the optical density of cell suspension was found to be increased with time, indicative of growth of bacteria. On the other hand, in the presence of CaO NPs optical density of bacterial cell suspension was decreased with the increase of CaO NPs with time. It clearly demonstrates that, the reduction of bacteria growth rate by increasing concentration of CaO NPs. At higher concentration of CaO NPs (50 μg ml^{-1}), the optical density was insignificant as the absorbance reaches the base line. It clearly suggests that there was no bacterial growth at this concentration. The minimum inhibitory concentration (MIC) of CaO NPs was found to be 10 μg ml^{-1} for both bacteria, respectively.

The antibacterial activity of CaO NPs against *E.coli* and *S.aureus* was also examined by measuring the diameter of inhibition zone (DIZ) using well disc diffusion method and the results are shown in Fig. S4. It can be clearly seen that, in the absence of CaO NPs (control experments), there was no inhibition zone. On the other hand, with the presence of CaO NPs, there was a clear formation of a inhibition zone, as no significant bacterial growth area

around the well present. The diameter of inhibition zone for Cao NPs against *E.coli* and *S.aureus* were found to be 19 ± 2 mm (Fig. S4A) and 17 ± 2 mm(Fig. S4B), respectively.

MALDI-MS has been used to investigate the antibacterial activity of nanoparticles by comparing proteins mass profile of treated and untreated (control) cells[17-19]. It provides not only accurate and clear protein mass profile for specific bacteria but also their changes in proteins mass profile after interaction with nanomaterials. Therefore, we have chosen MALDI-TOF MS as an important tool to investigate the antibacterial activity of CaO NPs to against the pathogenic bacteria. The samples of *E.coli* (Fig. 3A) and *S.aureus* (Fig. 3B) against variable concentration of CaO NPs (5, 10, 25, 50 μg mL^{-1}) after 12 h incubation time were analyzed using MALDI-MS. Further; we also collected bacterial MALDI-MS proteins profile without NPs treatment as a control experiment. In the case of lower concentration level (μg mL^{-1}), MALDI –MS proteins profile is similar to the control spectrum; it indicates that no cell death. But when the concentration was raised to 10 μg mL^{-1}, the number of protein peaks and their intensities were significantly reduced. The similar trend was continued upon further increasing the CaO NPs concentration up to 50 μg mL^{-1}. It's clearly demonstrates that the antibacterial activity of CaO NPs could effectively against pathogens bacteria by increasing the CaO concentration. In fact, at the highest concentration of 50 μg mL^{-1}, protein signals disappeared completely. The main reason for bacterial death is due to the degradation of cell walls or cell membranes to cleave surface associated proteins leading to less abundance of signals in the MALDI mass spectra. The signals may also be influenced by interaction and/or adsorption of the proteins with nanoparticles thereby depleting the intensity as well as number of signals in the mass spectra (Fig. 3). In addition the concentration of cell in suspension also may reason for changes in MALDI mass spectra protein profile.

The antibacterial activity of CaO NPs against *E.coli* and *S.aureus* were almost the same, which is well agreed with previous investigations[20-25]. The antibacterial action of CaO NPs is expected to dependent on the interactions between bacterial cells and CaO NPs. CaO NPs show adequate antibacterial activity due to high surface area to volume ratios, which not only provides good interaction with bacteria but also enhance reactive oxygen species (ROS) release on its surface. Sawai et al. and Hewitt et al. investigated that the generation of ROS is higher in alkaline pH due to dehydration of CaO NPs[21-24]. The ROS interact with carbonyl

group present in bacteria cell wall peptide linkages/polyunsaturated phospholipids and influence on proteins degradation consequently, leading to the destruction of bacteria cell wall.

In order to explain the interaction of bacterial cells and nanoparticles, TEM was performed in presence of CaO nano-plates (Fig S5). Fig S5A and Fig. S5C displays *E.coli* and *S.aureus* cells as control. Fig S5B and Fig. S5D shows death of bacterial cells after interaction with the nano-plates. It can be seen that the nano-plates accumulated around the cell membranes and inside the bacterial cells. Nano-plates must have entered inside the cells by disrupting cell membranes, which prove the mode of bactericidal activity of CaO nano-plates.

In summary, we demonstrate a novel green methodology for the synthesis of CaO nano-plates with length and width of ranging from 40 to130 nm and 30 to 100 nm. The developed method is rapid, facile, eco-friendly, economic and efficient green synthetic approach. The synthesized CaO nano-plates showed excellent antibacterial activity against gram positive and gram negative bacteria. The antibacterial activity is well demonstrated with optical density, well diffusion method and MALDI-MS. The green methodology appears to be alternative to traditional chemical and physical methods of CaO nanoparticles production. Therefore, it would be possible for developing a green approach for large-scale production of CaO nanoparticles for industrial purpose. CaO nanoparticles exhibit unique structural and optical properties, so they can be exploited in the near future for a variety of biomedical applications such as photodynamic therapy (PDT), photo-thermal therapy (PTT) and synaphic delivery of chemotherapeutic agents.

Acknowledgement:

We thank the ministry of science and technology (MOST) of Taiwan for financial support.

Figure caption

Figure 1. TEM images of CaO nanoplates (A) & (B) and particle size distribution histogram of CaO nanoplates (C) length & (D) width.

Figure 2. Effect of various concentrations of CaO nanoplates on bacterial growth at different time intervals (A) *E.coli* (B) *S.aureus.*

Figure 3. MALDI-MS proteins profile of pathogen bacteria acquired after incubation of 12h with various concentrations of CaO nanoplates (A) *E.coli* (B) *S.aureus.*

References

1. R. Ghosh Chaudhuri and S. Paria, *Chemical reviews*, 2011, 112, 2373-2433.
2. S. Sarkar, E. Guibal, F. Quignard and A. SenGupta, *Journal of Nanoparticle Research*, 2012, 14, 1-24.
3. M. J. Hajipour, K. M. Fromm, A. A. Ashkarran, D. J. de Aberasturi, I. R. de Larramendi, T. Rojo, V. Serpooshan, W. J. Parak and M. Mahmoudi, *Trends in biotechnology*, 2012, 30, 499-511.
4. P. T. Anh, T. T. M. Dieu, A. P. Mol, C. Kroeze and S. R. Bush, *Journal of Cleaner Production*, 2011, 19, 2107-2118.
5. R. H. Rødde, A. Einbu and K. M. Vårum, *Carbohydrate polymers*, 2008, 71, 388-393.
6. J. Zhang, W. Xia, P. Liu, Q. Cheng, T. Tahi, W. Gu and B. Li, *Marine drugs*, 2010, 8, 1962-1987.
7. M. Dash, F. Chiellini, R. M. Ottenbrite and E. Chiellini, *Progress in Polymer Science*, 2011, 36, 981-1014.
8. M. Teli and J. Sheikh, *International journal of biological macromolecules*, 2012, 50, 1195-1200.
9. A. Ghadami Jadval Ghadam and M. Idrees, *Iranian Journal of Chemistry and Chemical Engineering*, 2013, 32, 27-35.
10. R. K. Pai and S. Pillai, *CrystEngComm*, 2008, 10, 865-872.
11. M. Ghiasi and A. Malekzadeh, *Crystal Research and Technology*, 2012, 47, 471-478.
12. E. Mosaddegh and A. Hassankhani, *Chinese Journal of Catalysis*, 2014, 35, 351-356.
13. M. Mohammadi, P. Lahijani and A. R. Mohamed, *Chemical Engineering Journal*, 2014, 243, 455-464.
14. Y. Zhu, S. Wu and X. Wang, *Chemical Engineering Journal*, 2011, 175, 512-518.
15. V. K. Sharma, R. A. Yngard and Y. Lin, *Advances in colloid and interface science*, 2009, 145, 83-96.
16. V. Makarov, A. Love, O. Sinitsyna, S. M. I. Yaminsky, M. Taliansky and N. Kalinina, *Acta naturae*, 2014, 6, 35.
17. M. S. Khan, G. Gedda, J. Gopal and H.-F. Wu, *Analytical Methods*, 2014, 6, 5304-5313.
18. J. Gopal, H.-F. Wu and Y.-H. Lee, *Analytical chemistry*, 2010, 82, 9617-9621.
19. J. Gopal, M. Manikandan, N. Hasan, C. H. Lee and H. F. Wu, *Journal of Mass Spectrometry*, 2013, 48, 119-127.
20. A. Roy, S. S. Gauri, M. Bhattacharya and J. Bhattacharya, *Journal of biomedical nanotechnology*, 2013, 9, 1570-1578.
21. J. Sawai, *Journal of Microbiological Methods*, 2003, 54, 177-182.
22. J. Sawai, H. Shiga and H. Kojima, *International biodeterioration & biodegradation*, 2001, 47, 23-26.
23. J. Sawai and T. Yoshikawa, *Journal of applied microbiology*, 2004, 96, 803-809.
24. C. J. Hewitt, S. R. Bellara, A. Andreani, G. Nebe-von-Caron and C. M. McFarlane, *Biotechnology letters*, 2001, 23, 667-675.
25. D.-H. Bae, J.-H. Yeon, S.-Y. Park, D.-H. Lee and S.-D. Ha, *Archives of pharmacal research*, 2006, 29, 298-301.

The formation and characterization of Shrimp shells -derived CaO nanoplates for Antibacterial activity has been demonstrated in this communication.

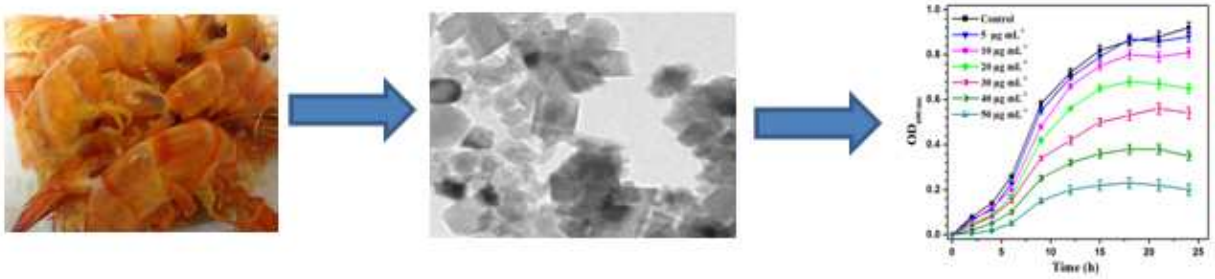

Shrimp shells **CaO nanoplates** **Antibacterial activity**